Monte Carlo study of the Villain version of the fully frustrated *XY* model

Peter Olsson*

Department of Theoretical Physics, Umeå University, 901 87 Umeå, Sweden
(Received 12 September 1996; revised manuscript received 22 October 1996)

The fully frustrated *XY* model with Villain interaction on a square lattice is studied by means of Monte Carlo simulations. On the basis of the universal jump condition it is argued that there are two distinct transitions, corresponding to the loss of *XY* order and Z_2 order, respectively. The Kosterlitz-Thouless (KT) transition is analyzed by finite-size scaling of the helicity modulus at lattices of size $L=32$ through 128, giving $T_{KT}\approx 0.8108(1)$. The vorticity-vorticity correlation function is used to determine two different characteristic lengths, the Z_2 correlation length ξ, and the screening length λ, associated with the KT transition and free vortices. The temperature dependence of ξ is examined in order to determine T_c and the correlation length exponent, ν. The exponent is found to be consistent with the two-dimensional (2D) Ising value, $\nu=1$, and the obtained critical temperature is $T_c=0.8225(5)$. The determinations of both ξ and ν are done carefully, first applying the techniques to the 2D Ising model, which serves as a convenient testing ground. [S0163-1829(97)00106-9]

I. INTRODUCTION

The critical behavior of the fully frustrated *XY* (FF*XY*) model has received much attention during the last decade. This is due to the two kinds of symmetries present in the systems and the associated possibility of new critical behavior. But in spite of the large number of papers, there is still no consensus about the phase transition(s) in this model.

The ordinary frustrated *XY* model (with cosines interaction) is governed by the Hamiltonian

$$H=-J\sum_{\langle ij\rangle}\cos(\theta_i-\theta_j-A_{ij}),$$

where i and j enumerate the lattice sites, θ_i is the angle at lattice point i, A_{ij} is the quenched vector potential, and the sum is over nearest neighbors. The frustration is determined by the sum of A_{ij} around a plaquette (see below). In the fully frustrated case—examined in the present paper—this sum is equal to π.

The peculiarities of the fully frustrated models stem from the two different symmetries. Beside the rotational symmetry of the *XY* model, the model also has a Z_2 symmetry associated with the chirality. The square-lattice version in the ground state has a checkerboard pattern of plaquettes with positive or negative chirality, corresponding to clockwise or counterclockwise rotation of the spins.[1] This is the same symmetry as in the antiferromagnetic Ising model.

Some other realizations of FF*XY* models are the antiferromagnetic *XY* model on a triangular lattice,[2] the Coulomb gas with half-integer charges,[3] and the 19-vertex version of the FF*XY* model.[4] All these models are generally assumed to have similar critical behavior. This is also expected to be true for the *XY* Ising model[5] for certain choices of some parameters.

In the first Monte Carlo (MC) simulations[6] Teitel and Jayaprakash found a divergence in the specific heat, consistent with an Ising transition, accompanied by a steep drop in the helicity modulus. But since the data did not allow for any precise determination of the critical temperature(s), the authors suggested two possible scenarios:

(1) At temperatures closely below T_c, the Ising excitations give rise to a steep drop in Υ. When Υ approaches $2T/\pi$, the vortex excitations take over and produce an universal jump at a temperature $T_{KT}<T_c$. This means two distinct transitions in well-known universality classes.

(2) The Ising excitations give a transition with an associated nonuniversal jump at the same temperature as the peak of the specific heat. This alternative is a single transition in a new universality class.

While these often have been considered the main options, several other possibilities have also been suggested in the literature, as, e.g., an Ising transition at a lower temperature than the Kosterlitz-Thouless (KT) transition.[7]

Over the years there have appeared several reports of MC studies where the losses of both *XY* and Z_2 orders have been studied. For the antiferromagnetic *XY* model on a triangular lattice,[2] a study of the heat capacity and the *XY* susceptibility suggested two distinct transitions, with $T_{KT}<T_c$. The temperature difference was, however, quite small and the possibility of a single transition could not be ruled out. In a second study of the same model,[8] including somewhat larger lattices and with a careful analysis of the Z_2 transition, the transitions were found to be even closer together. The temperature difference was in this study well below the statistical uncertainty. The results were therefore suggestive of a single critical point.

Likewise, there are conflicting results for the Coulomb gas with half-integer charges in the literature. A study by Thijssen and Knops[3] suggested coinciding transitions whereas Grest found two distinct transitions.[9] The conflicting values of the temperature for the loss of *XY* order was apparently due to different methods to locate the transition. In the first case T_{KT} was determined from the maximum finite-size dependence in $1/\epsilon$, and in the second case from the crossing of $1/\epsilon$ for different system sizes. The latter method gives a lower value of the transition temperature. The different results for the Z_2 transition seem to be due to differences

in the MC data. Whereas the earlier study reported a drift in position of the peak in the heat capacity to lower temperatures with increasing lattice size, such a size dependence was not verified in the latter simulation. This discrepancy gave higher values of T_c. Similar conclusions were also obtained from recent simulations of the Coulomb gas (CG) with half-integer charges.[10] The results from this study were two distinct transitions; at a lower temperature a KT transition with a nonuniversal jump, followed by a Z_2 transition with non-Ising exponents (see below).

As discussed in Ref. 11 the dielectric constant at smallest possible wave vector $k = 2\pi/L$ from the CG simulations, is not an ideal quantity for locating the KT transition. With this kind of boundary conditions, there are two finite-size effects working in the opposite directions. That this quantity is more or less size independent only means that these two effects happen to nearly cancel each other. This casts doubt on both the KT temperatures and the nonuniversal jumps found in the above studies.

In order to circumvent the difficulties associated with a precise determination of T_{KT} it has been argued that a determination of the critical exponents for the Z_2 transition by means of finite-size scaling, would be the best way to arrive at some firm conclusions. This, at first, seems a good idea since the study of finite-size effects right at T_c usually is the by far most efficient way to extract the critical behavior by MC simulations.

In this spirit the correlation length exponent ν, has been determined in a fairly large number of studies by means of finite-size scaling at T_c. In the MC simulations[12–14] this exponent is extracted from the temperature dependence of various kinds of measures of the distribution of the staggered magnetization. The same exponent has also been obtained from transfer-matrix calculations.[15] The results are generally in favor of non-Ising exponents, $\nu = 0.85(3)$, $0.813(5)$, $0.875(35)$, $0.80(4)$, and the critical temperatures $T_c/J = 0.455(2)$, $0.454(2)$, 0.4206, $0.454(4)$. Determinations of the same exponent in the 19-vertex version of the FFXY model,[4] the Coulomb gas with half-integer charges,[10] and the XY Ising model,[5,16] gave $\nu = 0.77(3)$, $0.84(3)$, $0.85(3)$, and 0.79, respectively. It seems, however, to be the case that such finite-size scalings in many cases are not quite satisfactory and are therefore not conclusive.[5,15,10]

With the steadily increasing computational resources it has been possible to obtain data with high precision for increasingly larger lattices. A recent paper reported results for the helicity modulus at a $L = 128$ system.[13] These data have far-reaching implications since it was shown that the helicity modulus crosses the universal line, $2T/\pi$, at a surprisingly low temperature, well below the temperatures quoted above for the Z_2 transition. This must be considered very strong evidence that the XY order is lost at a temperature below the T_c obtained from finite-size scaling; and thus excludes the single transition scenario. However, with this position the non-Ising exponents become problematic. The non-Ising exponents are usually explained as an effect of the interaction between XY and Ising critical excitations—a reasonable explanation only if the two kinds of order are lost at the same temperature.

We therefore have two pieces of evidence pointing in opposite directions. The presence of non-Ising exponents strongly suggests a single transition, whereas the early drop in the helicity modulus seems to exclude this possibility.

A consistent view of these matters was recently suggested in Ref. 17. The key observation is that a consequence of a KT transition below T_c would be the presence of a finite but large screening length λ, at the Z_2 transition temperature T_c. For finite-size scaling to be valid, it is necessary that L be much larger than all other finite length scales in the system, and in particular λ. The large value of λ could therefore invalidate earlier finite-size scaling analyses. The condition for a successful application of finite-size scaling at T_c, $L \gg \lambda$, may imply very large systems.

In the most ambitious study so far of the XY Ising model by means of Monte Carlo transfer-matrix calculations on infinite strips with widths up to 30 lattice spacings, Nightingale et al. again found evidence for non-Ising exponents.[16] They did, however, also find an ''internal inconsistency'' in two different determinations of the thermal exponent y_T, which led them to call in question the applicability of scaling theory. This inconsistency is certainly in line with the suggested failure of finite-size scaling due to the finite screening length λ.

The main results in Ref. 17 were a precise determination of T_{KT}, together with a demonstration that the staggered magnetization is, indeed, influenced by the screening length λ, unless $L \gg \lambda$, i.e., the helicity modulus $\Upsilon \approx 0$. In order to show that the behavior is consistent with the Ising exponent $\nu = 1$, the behavior of the correlation length was also examined. This part of the study was, however, hampered by two different complications. First, the correlation function did only fit nicely to an exponential decay for temperatures pretty far away from T_c. Second, it was difficult to include the effect of the spin waves in an entirely convincing manner. While it is certainly possible to argue in favor of the employed technique,[17] this is at best only an approximative way to compensate for the temperature-dependent effects of the spin waves.

One of the aims of the present study is to improve on the problematic points in the temperature dependence of the correlation length. The complications with temperature-dependent effects of the spin waves is taken care of by performing simulations in an FFXY model with Villain interaction—the model dual to the CG with half-integer charges. The point is that both the vortex interaction and the vorticity ($\pm 1/2$) are manifestly temperature independent in that model. To find a reliable technique for determinations of the correlation length, we compare with the behavior in the two-dimensional (2D) Ising model. In that case we benefit from the dual advantages of a fast cluster algorithm and exact knowledge of the critical behavior. From the simulations of the 2D Ising model we show that the region where the true Ising exponent may be found is very narrow. A similar analysis of the FFXY model gives the same kind of conclusion, and it therefore seems that the data points in Fig. 5 of Ref. 17 actually are outside the critical region.

The main result of the present analysis of the fully frustrated 2D XY model with Villain interaction is the existence of two distinct transitions. An ordinary Kosterlitz-Thouless transition at $T_{\mathrm{KT}}/J = 0.8108(1)$ followed by an Ising transition at $T_c/J = 0.8225(5)$, about 1.4% above. This is a fairly small temperature difference but, as we will see below, the

conclusion of two distinct transitions is not built on an estimate of the temperature difference between two separate transitions. Section III C 2. gives a strong argument for the existence of two transitions which is not based on the determinations of the two transition temperatures.

The organization of the present paper is as follows: In Sec. II we define the model, describe the quantities measured in the simulations and some of the analyses to be performed on the data. Section III begins our analyses of MC data. We shortly describe the MC procedure employed to obtain the data and some checks used to validate the results. The major part of Sec. III gives the results from various analyses that take advantage of the finite-size dependence in the MC data. Among these are the argument for two distinct transitions, the determination of T_{KT} through finite-size scaling of the helicity modulus, and an analysis of Binder's cumulant for the staggered magnetization.

Section IV contains the determinations of the characteristic lengths ξ and λ from the correlation function. In this paper ξ denotes the correlation length associated with the Ising-like degrees of freedom, whereas λ is the screening length associated with the KT transition, which (besides a constant factor) is equivalent to the XY correlation length. Since the finite-size effects in this context are unwanted complications, we take some pains to examine the appearance of finite-size effects. In order to test some techniques for the analysis of correlation functions, and the critical behavior from the correlation length, we make use of the 2D Ising model as a testing ground. After these preliminaries we employ these techniques to the correlation functions from the FFXY model to determine the temperature dependence of both ξ and λ above T_c, and ξ at low temperatures. Finally, in Sec. V we put our results in relation to some results by Bergé *et al.* for a model with a variable coupling for one link per plaquette,[18] and summarize our findings.

II. BACKGROUND

In this section we describe the model, discuss some quantities measured in the MC simulations and their relation to the more convenient Coulomb gas quantities, and shortly describe some analyses to be applied to the MC data.

A. Model

The model is defined through the partition function

$$Z = \int_0^{2\pi} \prod_i \frac{d\theta_i}{2\pi} e^{-\beta H},$$

where the Hamiltonian for a frustrated system is given by

$$H = \sum_{\langle ij \rangle} U(\theta_i - \theta_j - A_{ij}).$$

In the present case—the Villain version of the FFXY model—the spin interaction $U(\phi)$, is given by

$$e^{-\beta U(\phi)} = \sum_{n=-\infty}^{\infty} e^{-\beta J(\phi - 2\pi n)^2/2},$$

where ϕ is an angular difference between nearest neighbors. In the Hamiltonian above A_{ij} is the vector potential, and the frustration is given by the rotation of A_{ij}:

$$f_{\mathbf{r}} = \frac{1}{2\pi} \mathbf{D} \times \mathbf{A}_{\mathbf{r}} \equiv \frac{1}{2\pi} (A^y_{\mathbf{r}+\hat{\mathbf{x}}/2} - A^y_{\mathbf{r}-\hat{\mathbf{x}}/2} - A^x_{\mathbf{r}+\hat{\mathbf{y}}/2} + A^x_{\mathbf{r}-\hat{\mathbf{y}}/2}).$$

Full frustration, $f = 1/2$, may, e.g., be obtained by setting $A^y_{\mathbf{r}} = 0$ everywhere and $A^x_{\mathbf{r}} = \pi$ at every second row and zero otherwise. Here we introduce the discrete difference operator, $\mathbf{D} = (D_x, D_y)$, $D_\mu f_{\mathbf{r}} = f_{\mathbf{r}+\hat{\boldsymbol{\mu}}/2} - f_{\mathbf{r}-\hat{\boldsymbol{\mu}}/2}$, and A^x and A^y for the vector potential at links in the x and y directions, respectively. Associated with the discrete difference is $\tilde{k}$ which is obtained from

$$i\tilde{k}_x e^{i\mathbf{k}\cdot\mathbf{r}} = D_x e^{i\mathbf{k}\cdot\mathbf{r}} \Rightarrow \tilde{k}_x = 2\sin\frac{k_x}{2},$$

and also gives $\tilde{\mathbf{k}}^2 = 4 - 2\cos k_x - 2\cos k_y$.

B. Measured quantities

We now describe some of the quantities which are measured in the simulations, and are of central importance for the analyses in Secs. III and IV.

1. Helicity modulus

The helicity modulus Υ, is a measure of the quasi-long-range order in XY models. It is defined from the increase in free energy due to a small twist Δ across the system in one direction,

$$\Upsilon = \frac{\partial^2 F}{\partial \Delta^2}.$$

Written in this way, and with current $= \partial F/\partial \Delta$, the helicity modulus may be interpreted as the proportionality constant between the applied twist and the obtained macroscopic current. In MC simulations the helicity modulus is obtained from the correlation function[19]

$$\Upsilon = J_0 - \frac{\beta}{L^2} \left\langle \left(\sum_{\mathbf{r}} U'(\phi^x_{\mathbf{r}}) \right)^2 \right\rangle,$$

where $J_0 = \langle U''(\phi) \rangle$, and the sum in the second term is over all links in one direction, here the x direction.

2. Vorticity

Beside the helicity modulus the main quantity measured in our simulations is the Fourier transform of the vorticity. The vorticity is defined in terms of the rotation of the current $U'(\phi_{ij}) \equiv U'(\theta_i - \theta_j - A_{ij})$ around a plaquette,[2]

$$v = \frac{1}{2\pi J} [U'(\phi_{12}) + U'(\phi_{23}) + U'(\phi_{34}) + U'(\phi_{41})]. \tag{1}$$

The factor 2π in the denominator is chosen to give the zero-temperature limit $v = \pm 1/2$. This follows from the angular difference $\phi = \pm \pi/4$ in the ground state. The steps in the simulations consist of measuring $v_{\mathbf{r}}$ at each plaquette, Fourier transforming,

$$v_{\mathbf{k}} = \sum_{\mathbf{r}} v_{\mathbf{r}} e^{-i\mathbf{k}\cdot\mathbf{r}},$$

and accumulating the Fourier components squared, $|v_{\mathbf{k}}|^2$.

It is also common to define the vorticity in terms of the angular differences. That corresponds to the chirality, in the context of FFXY models. However, an appealing feature of the vorticity defined in Eq. (1) is that it is related to some derivatives of the free energy. This is also the reason for the existence of some *exact* relations between the measured vortex correlations and the correlations in the 2D CG with half-integer charges. The chirality, on the other hand, is somewhat peculiar in that it jumps discontinuously as a function of the angular differences.

3. The staggered magnetization

For the study of the Z_2 degrees of freedom associated with the symmetry of the antiferromagnetic Ising model, a convenient quantity is the staggered magnetization

$$M = \frac{2}{L^2} \left\langle \left| \sum_{\mathbf{r}} (-1)^{r_x+r_y} v_{\mathbf{r}} \right| \right\rangle, \tag{2}$$

where the sum is over all the plaquettes of the system, and the alternating sign is included to take care of the checkerboard pattern. The factor of $2/L^2$ is chosen to give $M=1$ in a well-ordered system. In an infinite system this quantity has a finite value in the low-temperature phase and goes to zero as T_c is approached from below, but this sharp behavior is considerably smoothed in the finite systems of the MC simulations. Since $(-1)^{r_x+r_y} = e^{-i(\pi,\pi)\cdot\mathbf{r}}$, M is directly related to the $\mathbf{k}=(\pi,\pi)$ component of the vorticity. Also useful are some powers of the staggered magnetization,

$$M^p = \left(\frac{2}{L^2} \sum_{\mathbf{r}} (-1)^{r_x+r_y} v_{\mathbf{r}} \right)^p.$$

Binder's cumulant in Sec. II E is defined from $\langle M^2 \rangle$ and $\langle M^4 \rangle$.

C. Duality relation and the correlation function

It has been argued that both the vortex interaction and the average vorticity at a plaquette are temperature dependent in the FFXY model with cosines interaction.[17] To avoid this kind of complicating factors one would rather have results from the CG with half-integer charges, since both the average vorticity and the vortex interaction in that model are manifestly temperature independent. However, since simulations of that model are considerably more time-consuming, we instead perform simulations of the spin model with the Villain interaction, and make use of an *exact* relation between the measured vorticity correlations and the corresponding correlations for the CG half-integer charges. In this section we shortly discuss the duality transformation, define the Z_2 correlation function, $g(\mathbf{r})$ and $g(\mathbf{k})$, and derive the link between our measured vorticity correlations and $g(\mathbf{k})$.

In the Appendix we discuss the duality transformation[20,21] applied to the FFXY model. This gives the Hamiltonian

$$H^{\mathrm{CG}} = -4\pi^2 J \frac{1}{2} \sum_{\mathbf{r},\mathbf{r}'} m_{\mathbf{r}} G(\mathbf{r}-\mathbf{r}') m_{\mathbf{r}'}, \tag{3}$$

where $m_{\mathbf{r}}$ are half-integer charges, $m_{\mathbf{r}} = \pm 1/2, \pm 3/2, \ldots$, and $G(r)$—the lattices Green's function—is the solution to $\mathbf{D}\cdot G(\mathbf{r}) = \delta_{\mathbf{r}}$, with $G(0)=0$ and proper boundary conditions. An excellent approximation for $r \geqslant 1$ is $2\pi G(r) = \ln r + \mathrm{const}$.

It is now convenient to define the Z_2 correlation function in terms of the CG charges $m_{\mathbf{r}}$. For the correlation function in ordinary space we write,

$$g(\mathbf{r}) = 4(-1)^{r_x+r_y} \langle m_0 m_{\mathbf{r}} \rangle, \tag{4}$$

where the prefactors, again, are for normalization and the checkerboard pattern in the well-ordered ground state. In the low-temperature phase this quantity has a finite value in the $r \to \infty$ limit, whereas it approaches zero above T_c. The approaches to these limits are exponential, governed by the correlation length ξ. As discussed below, the correlation length is, however, better determined from the Fourier components $g(\mathbf{k})$.

The Fourier expansion of the correlation function is

$$g(\mathbf{r}) = \frac{1}{L^2} \sum_{\mathbf{k}} g(\mathbf{k}) e^{i\mathbf{k}\cdot\mathbf{r}} = (-1)^{r_x+r_y} \frac{1}{L^2} \sum_{\mathbf{q}} g(\mathbf{q}) e^{i\mathbf{q}\cdot\mathbf{r}},$$

where we introduce $\mathbf{q} = (\pi,\pi) - \mathbf{k}$ and $g(\mathbf{q})$. Together with Eq. (4) this gives

$$g(\mathbf{k}) = \frac{4}{L^2} \langle m_{\mathbf{k}} m_{-\mathbf{k}} \rangle. \tag{5}$$

A link between the vorticity correlation function and the corresponding correlation function of CG charges may be obtained by considering two different expressions for the wave-vector dependent helicity modulus $\Upsilon(\mathbf{k})$, which is equivalent to the dielectric function $J/\epsilon(\mathbf{k})$.[22] In the Coulomb gas picture, with the interaction $4\pi^2 J G(r) \sim 2\pi J \ln r$, $\Upsilon(\mathbf{k})$ becomes

$$\Upsilon(\mathbf{k}) = J - \frac{4\pi^2 J^2}{TL^2 \widetilde{\mathbf{k}}^2} \langle m_{\mathbf{k}} m_{-\mathbf{k}} \rangle, \tag{6}$$

whereas the same quantity in the XY variables is

$$\Upsilon(\mathbf{k}) = J_0 - \frac{4\pi^2 J^2}{TL^2 \widetilde{\mathbf{k}}^2} \langle v_{\mathbf{k}} v_{-\mathbf{k}} \rangle. \tag{7}$$

In the Appendix we show that these two expressions are the same derivative of the free energy, which means that they have to be equal. This gives the desired link between the correlation functions for our measured vorticity and the half-integer variables of the CG model,

$$\langle m_{\mathbf{k}} m_{-\mathbf{k}} \rangle = \langle v_{\mathbf{k}} v_{-\mathbf{k}} \rangle + \frac{T(J-J_0)}{J^2} \frac{L^2 \widetilde{\mathbf{k}}^2}{4\pi^2}. \tag{8}$$

Together with Eq. (5) this gives the desired expression for the correlation function $g(\mathbf{k})$ in terms of the measured correlations $\langle v_{\mathbf{k}} v_{-\mathbf{k}} \rangle$. This is the procedure used to determine $g(\mathbf{k})$ which is analyzed in Sec. IV.

The last term in Eq. (8) is under certain conditions very small beside the vorticity correlation term $\langle v_{\mathbf{k}} v_{-\mathbf{k}} \rangle$. This is especially the case at $\mathbf{q} \approx 0$ for temperatures around T_c, which means that the determinations of ξ and ν in Sec. IV would be influenced only very slightly by neglecting this correction.

The relation between the CG correlations and the vorticity correlations in ordinary space has been discussed in Ref. 21. For the case with the Villain spin interaction the result was $\langle m_0 m_{\mathbf{r}} \rangle = \langle v_0 v_{\mathbf{r}} \rangle$. However, as seen in their derivation this holds for $|\mathbf{r}| > 1$, only. For general $\mathbf{r}$ the Fourier transform of Eq. (8) gives

$$\langle m_0 m_{\mathbf{r}} \rangle - \langle v_0 v_{\mathbf{r}} \rangle = \begin{cases} 4T(J-J_0)/(2\pi J)^2, & \text{if} \quad \mathbf{r}=0, \\ -T(J-J_0)/(2\pi J)^2, & \text{if} \quad |\mathbf{r}|=1, \\ 0, & \text{otherwise.} \end{cases} \tag{9}$$

In Sec. III B the above relation for $\mathbf{r}=0$ is used in a consistency check.

D. Analysis of Υ

In this section we discuss the size dependence of the helicity modulus Υ and its relation to the universal jump and Kosterlitz' renormalization-group (RG) equations. We will focus on the dimensionless quantity T/Υ.

For the finite-size scaling analysis of T/Υ one assumes that the size dependence in this quantity is related to the behavior of a set of RG trajectories.[23] The starting point in parameter space, and thereby the relevant trajectory, is determined by the temperature. These trajectories behave differently in the low- and high-temperature phases. In the low-temperature phase they terminate at finite values of T/Υ whereas they continue to infinity, corresponding to $\Upsilon \rightarrow 0$, in the high-temperature phase.

The last trajectory in the low-temperature phase ends at the universal value $T^{CG}/\Upsilon \equiv T/(2\pi\Upsilon) = 1/4$. This means that the helicity modulus for that very temperature in an infinite system is $\Upsilon = 2T/\pi$. The jump of this quantity to zero is the well-known universal jump.[24,25]

The abrupt universal jump of an infinite system is, of course, not seen in finite systems. Since Υ decreases with increasing system size, the universal jump conditions $\Upsilon = 2T/\pi$ may, however, be used to establish an upper limit for T_{KT}. The temperature obtained in that way is a rigorous upper limit, since the universal jump condition constitutes an absolute stability criterion.

The approach to the universal value, $\Upsilon \pi/(2T) = 1$, with increasing system size, may also be used to examine the critical properties. From Kosterlitz' RG equations[23] the finite-size scaling relation for Υ_L becomes[26]

$$\frac{\Upsilon_L \pi}{2T} = 1 + \frac{1}{2(\ln L + l_0)}. \tag{10}$$

Kosterlitz' RG equations are expected to be valid only in the limit of low vortex density. This means that the above finite-size scaling relation is expected to be valid only at low renormalized vortex density. Accordingly, $\Upsilon_L \pi/(2T)$ should be not too far from unity—Υ renormalized out to length scale

L should not be too far from the fully renormalized Υ out to infinity. This implies the dilute limit for sizes bigger than L.

The same idea may also be used both above and below T_{KT}. A more complete discussion is given in Ref. 27. Close to T_{KT} we expect[22,27]

$$\frac{\Upsilon_L \pi}{2T} = 1 + c\coth[2c(l_0 + \ln L)], \quad T<T_c, \tag{11}$$

$$\frac{\Upsilon_L \pi}{2T} = 1 - c\cot[2c(l_0 - \ln L)], \quad T>T_c, \tag{12}$$

where l_0 and c are free parameters to be determined from the fits. Equation (10) is the $c \rightarrow 0$ limit of Eq. (11). c vanishes as T_{KT} is approached from below or above as[23]

$$c = B\sqrt{|T/T_{KT}-1|}. \tag{13}$$

In the high-temperature phase l_0 is identified with the logarithm of the screening length, λ. In the immediate vicinity of T_{KT} the temperature dependence of l_0 should therefore be given by Kosterlitz' expression[23]

$$l_0 = \frac{C}{\sqrt{T/T_{KT}-1}} + \text{const}, \tag{14}$$

where[22]

$$C = \frac{\pi}{2B}. \tag{15}$$

E. Binder's cumulant

Binders' cumulant is a convenient quantity that, in most cases, facilitates determinations of both the critical temperature and the correlation length exponent ν. Even though the quantity was originally presented in terms of averages over blocks of different size in a single simulation with a fixed total system size,[28] it may also be used with data from systems of different size. Binder's cumulant is obtained from some moments of the order parameter,

$$U = 1 - \frac{\langle M^4 \rangle}{3\langle M^2 \rangle^2}. \tag{16}$$

The crucial property of U is its size independence precisely at T_c. Therefore, plotting U versus temperature for several different sizes is expected to give a unique crossing point at the critical temperature. Furthermore, the correlation length exponent ν may be determined by plotting the data against $(T-T_c)L^{1/\nu}$. The correct value of ν is expected to give a collapse of that data onto a single curve. In practice there are, however, often corrections to scaling which make the conclusions from this kind of analysis less direct and precise.

F. Boundary conditions

It has recently been pointed out that periodic boundary conditions (PBC's) in the XY model may be generalized by including twist fluctuations along the x and y directions in the system—fluctuating boundary conditions (FBC's).[29,11] There are several advantages with considering such a gener-
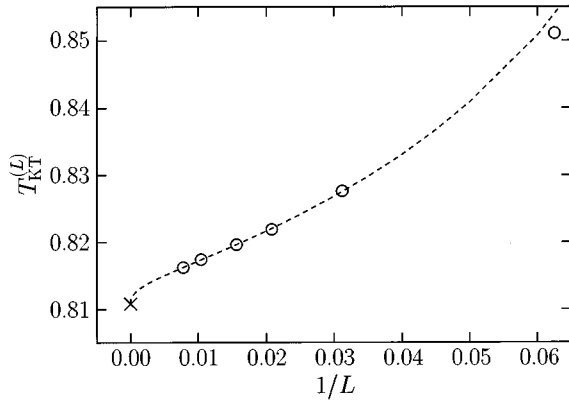
FIG. 1. The size dependence of $T_{\mathrm{KT}}^{(L)}$. The cross is T_{KT} from Sec. III D and the dashed line is from the analysis in Sec. III E.

alization. First, it is with these boundary conditions that the Villain version of the XY model is exactly dual to the CG with periodic boundary conditions. Second, the finite-size effects in several quantities work in the opposite way after the inclusion of these twists. Finally, with a self-consistently chosen amplitude of these twists, the finite-size effect on the correlation function turns out to be virtually eliminated.

The self-consistent boundary conditions do not seem to be applicable in the fully frustrated case. This is possibly an effect of the Z_2 fluctuations. It is, however, possible to obtain the correlation function as in an infinite system by taking the average of data for PBC's and FBC's, cf. Fig. 1 in Ref. 29. This technique works up to, and possibly slightly above T_{KT}. At higher temperatures both sets of data go down with increasing lattice size, which makes it considerably more difficult to extract any result for the thermodynamic limit.

III. FINITE-SIZE ANALYSES

The different methods to analyze MC data may, generally speaking, be divided into two classes. The most obvious one is to calculate the correlation functions and determine the correlation length and the associated exponents from this kind of data. In this kind of analyses one is interested in the behavior of an infinite system and, accordingly, the finite-size effects are undesired complications. This kind of analyses is the subject of Sec. IV.

The second class of methods instead *take advantage* of the finite-size dependence in the MC data. This is generally a more efficient approach to analyzing the critical behavior. In this section we employ some techniques that make use of the finite-size dependence in various ways.

After a short description of the simulations and some checks employed to validate the results, we focus on results from the universal jump condition in Sec. III C. In Sec. III D we perform finite-size scaling analyses of the helicity modulus Υ both right at T_{KT} and in the immediate neighborhood around T_{KT}. With this determined value for T_{KT} we then take a closer look at the data from the universal jump condition in Sec. III E.

To obtain a reference temperature we then apply finite-size scaling analysis of Binder's cumulant at T_c. Just as in the related models this kind of analysis gives $\nu < 1$. As sug-

gested in Ref. 17 this seems to be an artifact of the presence of a finite screening length λ associated with the nearby KT transition.

A. Monte Carlo simulations

The Monte Carlo simulations were performed with the ordinary Metropolis algorithm with sequential sweeps over the lattices. One such sweep with one trial update per spin is called a MC step. For most of the data there were four MC steps between consecutive measurements. But since it was noted that a major part of the computer time, especially on the large lattices, was used in the fast Fourier transform of the measured vorticity $v_{\mathbf{r}}$, the simulations for $L = 128$ and 256 for determinations of ξ were performed with as much as 64 MC steps between consecutive measurements. For the latter data the number of MC steps are given in Table II.

In Sec. IV we make use of MC data from the 2D Ising model as a convenient testing ground for the methods used to analyze the FFXY model. These simulations were performed with Wolff's cluster algorithm.[30] All the simulations were done on a set of DEC-alpha workstations.

B. Monte Carlo data

A MC study is, of course, never more reliable than the underlying data. It is therefore essential to check that the program, indeed, does provide correct data. This may be done either by comparing with previously published results or by making use of some consistency tests.

To the best of our knowledge there is no published MC data to compare with for the Villain version of the fully frustrated XY model with ordinary PBC's. For the case with FBC's it is, however, possible to compare with data for the half-integer CG.[10] For $L = 8$ and $T/J = 0.82$ our simulations give Binder's cumulant, $U = 0.5786$. This temperature corresponds to $T^{\mathrm{CG}} = 0.1305$, and as expected our value for U lies right in-between the values for U at $T^{\mathrm{CG}} = 0.130$ and 0.131 in Fig. 3 of Ref. 10. As a second test we compare the values of $\Upsilon(k = 2\pi/L)$ for $L = 16$ and $T/J = 0.82$. Again, the value obtained from our simulations, 0.556 788, is in good agreement with the corresponding values in Fig. 4 of Ref. 10.

For the bulk of our data, obtained with ordinary PBC's we have to resort to internal consistency tests. One such test is suggested by the analogy with the CG with half-integer charges. In that case, the charges $m = \pm 1/2$ give $\langle m^2 \rangle = 1/4$. Actually, the value 1/4 turns out to be a lower bound since the CG also includes charges of nonlowest order, i.e., $m = \pm 3/2$.[31] For our measured quantity v^2, there is no such simple result, but as discussed above there is an exact relation between these two quantities, Eq. (9).

Whereas $\langle v^2 \rangle$ decreases with increasing temperature to about 2.5% below 1/4 at $T/J = 0.9$ we find that $\langle m^2 \rangle$ stays close to 1/4. More precisely, the results are $\langle m^2 \rangle = 0.250\,000$ at $T/J = 0.4$, $0.250\,003$ at $T/J = 0.77$, and $0.250\,078$ at $T/J = 0.9$. This constitutes a confirmation of the correctness of the MC data. From the minute deviations of $\langle m^2 \rangle$ from 1/4 it is also possible to obtain estimates of the fraction of plaquettes with nonlowest order charges in an equivalent CG. For the temperature interval $T/J = 0.77$ through 0.9 our data indicates that this fraction is from 1.5×10^{-6} to 39×10^{-6}.

C. Universal jump condition

In this section we make use of the universal jump condition to obtain both an upper limit of T_{KT} and a strong evidence in favor of two distinct transitions. Since the universal jump condition is an absolute stability requirement, we believe the argument of the present section to be especially free of objections. Whereas the more precise results in the later sections are obtained on the basis of additional assumptions, the direct use of the universal jump condition is particularly clean. For the following discussion we introduce the size-dependent transition temperature $T_{KT}^{(L)}$, as the temperature where the helicity modulus for system size L is equal to the universal value, $\Upsilon_L = 2T_{KT}^{(L)}/\pi$.

1. Upper limit of T_{KT}

The universal jump condition was applied to the fully frustrated XY model with cosines interaction in Ref. 13 to establish an upper limit for the KT temperature. From the intersection of the MC data for $L=128$ with the universal value, these authors found, as discussed in the Introduction, $T_{KT}^{(128)}/J = 0.449(1)J$, clearly below the values of T_c determined with finite-size scaling.

The same approach with the data for the Villain version gives $T_{KT}^{(128)} \approx 0.816J$ as the upper limit for $L=128$. Figure 1 shows the size dependence of $T_{KT}^{(L)}$. The dashed line is from the analysis in Sec. III E.

2. Two transitions

We now turn to the argument for two distinct transitions based solely on the universal jump condition.[24,25] The argument has also been briefly presented in Ref. 32 where it was applied to the cosines version of the FFXY model.

The starting point is that the staggered magnetization for an infinite system, M_∞, vanishes at the Z_2 transition temperature T_c. To establish the existence of two distinct transitions it is therefore sufficient to examine M_∞ right at T_{KT}. A nonzero value of $M_\infty(T_{KT})$ would be an unequivocal demonstration of Ising order, which then implies that this order is lost at a higher temperature, $T_c > T_{KT}$. The determination of $M_\infty(T_{KT})$ at first seems very difficult since, beside the usual problem of approaching the thermodynamic limit, the value of T_{KT} has to be known with high precision. The universal jump criterion used so far, is only capable of yielding upper limits.

A way around both these difficulties at the same time is to focus on $M_L(T_{KT}^{(L)})$, the staggered magnetization of finite lattices at the size-dependent KT temperatures, and examine the behavior of this quantity as a function of system size, L. The point is that the desired quantity $M_\infty(T_{KT})$ is the large-L limit of $M_L(T_{KT}^{(L)})$, and that the staggered magnetization is readily determined by simulations for various system sizes, L.

The results from this analysis are shown in Fig. 2. The figure shows that the staggered magnetization at $T_{KT}^{(L)}$ is an *increasing* function of lattice size. The figure gives 0.744 as a lower limit of $M_\infty(T_{KT})$, and a naive extrapolation, that neglects the curvature, suggests $M_\infty(T_{KT}) > 0.768$.

We consider this to be a very strong argument that the Z_2 order persists at the KT transition temperature. For the
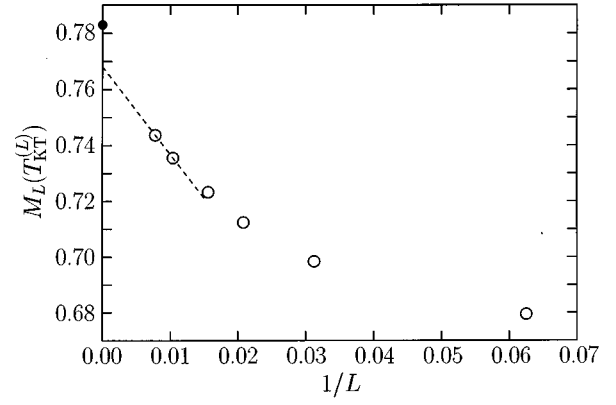

FIG. 2. Evidence for two distinct transitions. The plotted quantity is known to approach $M_\infty(T_{KT})$ in the limit $L \to \infty$. The dashed line shows a naive extrapolation, whereas the dot is this quantity from Sec. IV E obtained with the value of T_{KT} from Sec. III D.

opposite to be true, this increasing trend toward a finite value of $M_\infty(T_{KT})$ should change to a decreasing trend down to zero. Even though this possibility could never be ruled out from the data for finite systems alone, such a change in trend seems very unlikely. Furthermore, the more detailed analysis in the following sections yields $M_\infty(T_{KT}) = 0.783(2)$, entirely consistent with the increasing trend in Fig. 2. It should also be noted that this line of evidence does not depend on the assumption of a *universal* jump. The argument holds equally well with a jump $\Upsilon \pi/(2T) = g$, $g > 1$. ($g < 1$ is excluded by stability.)

D. Kosterlitz-Thouless transition

The purpose of this section is first to determine the Kosterlitz-Thouless temperature, T_{KT}, and, second, to examine the behavior closely below and above this temperature. The method employed is finite-size scaling analysis of the helicity modulus as discussed in Sec. II D. The basic idea is that the size dependence of the helicity modulus Υ, at and in the vicinity of T_{KT}, may be obtained from Kosterlitz RG equations[23] as given by Eqs. (10), (11), and (12).

The analysis of the helicity modulus Υ, is based on a large amount of MC data. In order to make efficient use of the data and get Υ_L as continuous functions of T, we first determine the helicity modulus as second-order polynomials, one for each L, in $\tau = T/J - 0.8107$:

$$\frac{\Upsilon_L \pi}{2T} = \alpha_L + \beta_L \tau + \gamma_L \tau^2. \tag{17}$$

These second-order expansions are only expected to be valid within rather narrow temperature intervals. We therefore only include data in the fits for temperatures $|\tau| < T_{range}/J$, where T_{range} decreases with increasing L. The parameters from this analysis together with the size of the temperature intervals are shown in Table I.

1. Determination of T_{KT}

We now apply the finite-size scaling relations for the helicity modulus as discussed in Sec. II D. Since the relations in this system only are expected to be valid for fairly large

TABLE I. Parameters from fitting MC data for the helicity modulus to Eq. (17). The data included in the fits are restricted to $|T/J - 0.8107| < T_{\text{range}}/J$.

L	α_L	β_L	γ_L	T_{range}/J
16	1.3932(17)	-8.545	-19.9	0.021
24	1.3179(20)	-11.06	-143.6	0.015
32	1.2731(12)	-12.86	-207.4	0.01
48	1.2235(13)	-15.75	-190.8	0.008
64	1.1989(13)	-17.55	-352.1	0.0065
96	1.1714(15)	-20.20	-439.0	0.0051
128	1.1578(20)	-21.30	-304.1	0.0045

lattices we first follow the procedure in Ref. 27 and perform the analysis with systems of size $L = L_{\min}$ through 128 and various values for $L_{\min}$. The errors in the fits are shown in Fig. 3. On the basis of this analysis we conclude that $L_{\min} = 32$ does give a good fit. This is the same choice as for the FFXY model with cosines interaction in Ref. 17.

Figure 4 shows the good fit of the MC data to Eq. (10) obtained by adjusting T_{KT} and l_0. The obtained value for the KT temperature is $T_{\text{KT}}/J = 0.8108(1)$. We consider the good fit to Eq. (10) to be very strong evidence for an ordinary KT transition.

Note that $T_{\text{KT}}/J = 0.8108$ is well below the upper limit $T/J = 0.816$ from the universal jump criterion in Fig. 3. It is also slightly lower than what a simple linear extrapolation of the four lowest points to $1/L = 0$ in Fig. 1 would suggest.

2. Finite-size scaling around T_{KT}

We now shortly discuss the critical behavior in the immediate vicinity of T_{KT}. The approach closely follows Ref. 27.

In fitting our MC data to Eqs. (11) and (12) we fix the temperature, calculate $\Upsilon_L \pi/(2T)$ from the parameters in Table I and adjust c and l_0 to get the best possible fit. In the high-temperature phase, l_0 is the logarithm of the screening length, λ. Below T_{KT} this quantity has no such direct interpretation. The parameter B in Eq. (13) may then be obtained
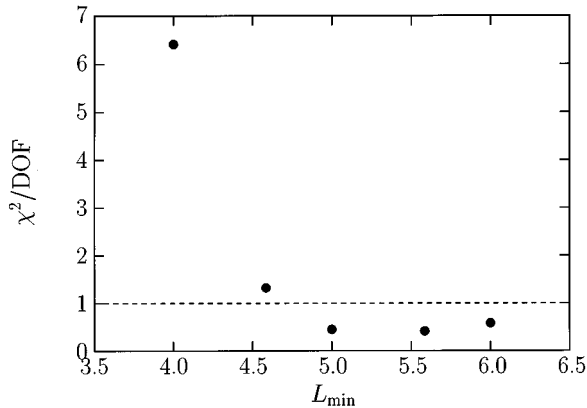

FIG. 3. The quality of the fit from fitting Υ_L to Eq. (10). $L_{\min}$ is the smallest size included in the fit. For a good fit one expects $\chi^2/\text{degree of freedom} \approx 1$. The figure indicates that the fit is not very successful when including small lattices, but becomes acceptable for $L_{\min} = 32$.
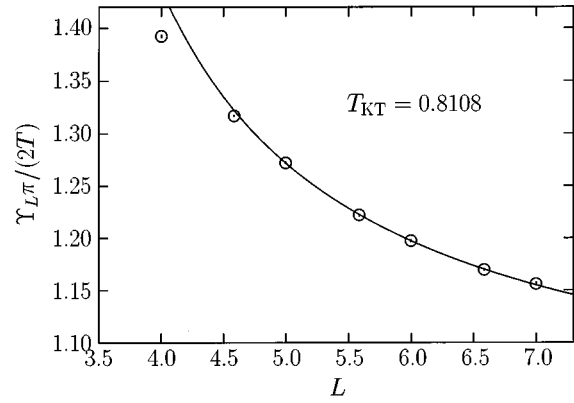

FIG. 4. Υ_L versus lattice size for $T_{\text{KT}} = 0.8108J$. The solid line is Eq. (10) with $l_0 = -1.63$. The good fit is strong evidence for an ordinary KT transition.

from the temperature dependence of c. Just as in the analysis of the ordinary XY model the values of the parameters B obtained from the low- and high-temperature data are, within statistical errors, the same, $B = 2.889$ and 2.834, respectively. Through Eq. (15) this gives $C = 0.544$ and 0.554 for the slope of the logarithm of the characteristic length. The slope C may also be obtained directly from the temperature dependence of l_0. In this way we arrive at $C = 0.532$, and our final estimate for the slope becomes $C = 0.54 \pm 0.02$.

In Secs. III E and IV D we will obtain different values for C, but we consider the present determination to be the more reliable one for two reasons. First, it does build on excellent agreements with predictions from the Kosterlitz' RG equations and, second, in contrast to other determinations, this method does probe the behavior in the immediate vicinity of T_{KT}.

E. Size dependence of $T_{KT}^{(L)}$

In Sec. III C we made use of the universal jump condition to determine a kind of size-dependent KT temperatures $T_{\text{KT}}^{(L)}$ as upper bounds for T_{KT}. From Fig. 1, it seemed difficult to extrapolate such data to the thermodynamic limit.

We now demonstrate that the size dependence of $T_{\text{KT}}^{(L)}$ has the same form as the Kosterlitz' expression for the temperature dependence of the correlation length, i.e.,

$$\ln L = \text{const} + \frac{C'}{\sqrt{T_{\text{KT}}^{(L)}/T_{\text{KT}} - 1}}. \tag{18}$$

Figure 5 shows the approach of $T_{\text{KT}}^{(L)}$ to $T_{\text{KT}} = 0.8108J$ with increasing L. The points do, indeed, fall on a straight line. This is the same dashed line as in Fig. 1. It should be noted that it does not seem possible to link this behavior directly to the divergence of the screening length λ. In the present approach the slope is $C' \approx 0.265$, whereas the same constant in the temperature dependence of l_0 yielded $C \approx 0.54$ which is about twice as big.

This size dependence of $T_{\text{KT}}^{(L)}$ is also found in the ordinary 2D XY model with no frustration. Here the slope is found to
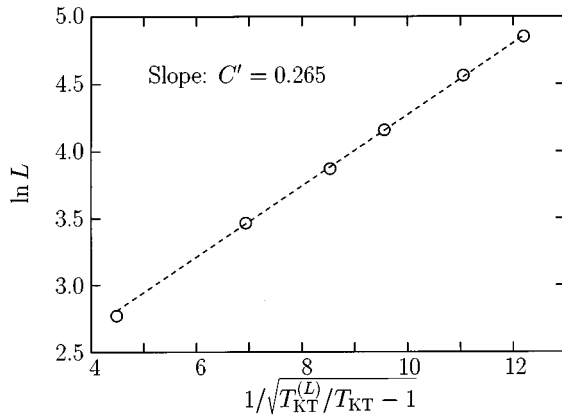
FIG. 5. The size dependence of $T_{\mathrm{KT}}^{(L)}$ for the FFXY model, with lattice sizes $L = 16$, 32, 48, 64, 96, and 128. The value for the transition temperature is taken from the determination in Sec. III D. Note that the slope C' is entirely different from the corresponding slopes from the temperature dependence of the screening length.

be ≈ 0.85, and, again, the temperature dependence of the characteristic length gives a slope that is about two times as big.[33]

F. Binder's cumulant

As discussed in the Introduction the existence of two transitions close to each other may give rise to problems with ordinary finite-size scaling. The evidence for the two transitions given in the previous section strongly implies that this actually is the case for the FFXY model. This means that the critical properties are not accessible with finite-size scaling at T_c unless the systems employed are considerably larger than the correlation length associated with the other (here the KT) transition.

The purpose of the present finite-size scaling analysis is therefore not to extract the correct critical behavior, but rather to provide a reference temperature and to verify that the FFXY model with Villain interaction indeed does behave in a way that is similar to the more studied FFXY model with cosines interaction.

Figure 6(a) shows Binder's cumulant versus temperature for $L = 8$, 16, 32, and 64. As discussed in Sec. II E, U is expected to be size-independent right at the critical temperature. This is not quite borne out by the data. A close look reveals that the crossing points move slowly to lower temperatures for larger system sizes. For the pairs of lattice sizes $L = 8$, 16, $L = 16$, 32, and $L = 32$, 64, the crossing temperatures are 0.827, 0.825, and 0.824, respectively, though the two last temperatures are within the statistical uncertainties. This is in good agreement with $2\pi \times 0.1315(3) = 0.826(2)$ obtained from simulations of the CG with half-integer charges on lattices with size $L = 10 - 24$ in Ref. 10. Since the ordinary periodic boundary conditions in that simulation corresponds to FBC's in spin models (cf. Sec. II F), whereas the present simulations are performed with PBC's, the value of the cumulant at criticality is, however, not expected to be the same.[17]

Figure 6(b) shows the data collapse. Following Ref. 10 we assume that $U_L(T) = \phi(tL^{1/\nu})$, where $t = T/T_c - 1$. We then expand $\phi(x) = \phi_0 + \phi_1 x + \phi_2 x^2$ for small x and adjust
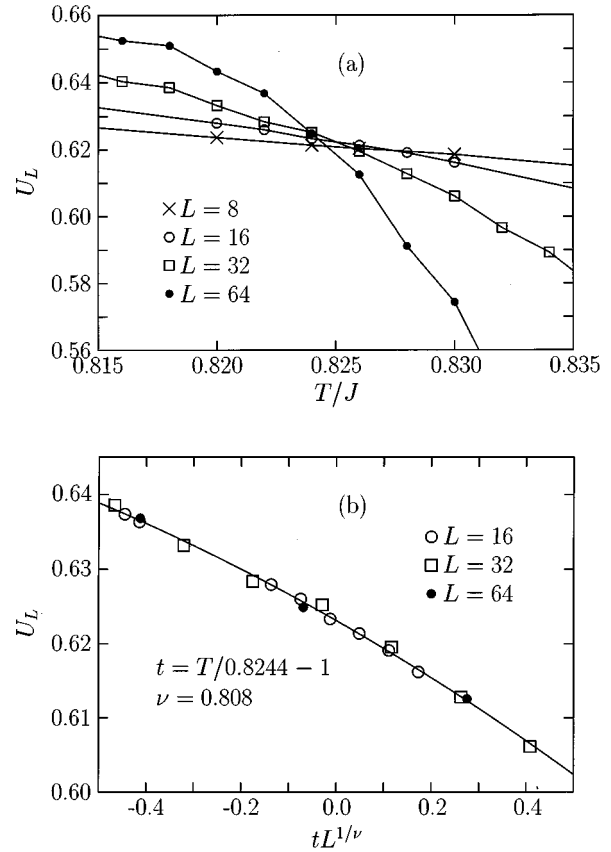

FIG. 6. Binder's cumulant U_L for different lattice sizes. (a) U is more or less size independent for $L \geq 16$ at $T/J \approx 0.824$. (b) An attempted data collapse. Just as in the FFXY model with cosines interaction this kind of analysis suggests $\nu < 1$.

these three parameters together with ν and T_c to get the best possible fit. With data close to T_c, $(0.605 < U < 0.640)$ for system sizes $L = 16$, 32, and 64, we obtain $T_c = 0.8244$ and $\nu \approx 0.81$. This value of ν is in good agreement with the published values, listed in the Introduction.

IV. CORRELATION LENGTHS

In the previous section we performed a number of analyses with methods that take advantage of the finite-size effects in the MC data. This is usually the most efficient way to determine the critical behavior from Monte Carlo simulations. The alternative approach is to determine the correlation length from the length dependence of some correlation functions and then extract the critical behavior from its temperature dependence. In the present section we take this alternative route.

In order to test some techniques for determining the correlation length and extracting the correlation length exponent and the critical temperature, we first present an analysis of the 2D Ising model. Because of the dual advantage of a known critical behavior and a fast cluster update algorithm, this model serves as a very convenient testing ground. One minor difference between the analysis of the 2D Ising model and the FFXY model is due to the antiferromagnetic ordering. Whereas the critical behavior of the ferromagnetic Ising model is obtained in the $k \to 0$ limit, the corresponding criti-

cal behavior in the FFXY model manifests itself at $\mathbf{k}=(\pi,\pi)$. This is taken care of by performing all the analyses in Sec. IV C in terms of $\mathbf{q}=(\pi,\pi)-\mathbf{k}$ instead of $\mathbf{k}$, cf. Sec. II C.

In this section we determine two different characteristic lengths from our MC data for $\langle v_{\mathbf{k}}v_{-\mathbf{k}}\rangle$. The reason that it is at all possible to define *two different* characteristic lengths is related to the above discussion. Whereas the screening length λ is determined from the $k\to0$ limit of these correlations, the correlation length ξ is determined from the limit $q\to0$.

For the determination of the characteristic lengths one would like to have the correlation function for an infinite system. It is therefore of great importance to know when the undesired effects of the finite lattice size set in. Before applying the obtained techniques to the FFXY model we do a careful analysis of the finite-size effects in this model. The results corroborate the suggestion[17] that the correlation function is plagued by finite-size effects unless the system is large enough that $\Upsilon\approx0$.

After these preliminaries we then turn to determinations of the correlation length ξ, the critical exponent ν, and the critical temperature T_c, in the FFXY model. Much as expected from the evidence of two distinct transitions, the behavior is found to be consistent with an ordinary Ising transition, $\nu=1$. However, for this demonstration it turns out to be necessary to examine the behavior fairly close to T_c, which corresponds to large correlation lengths, $\xi>10$. The screening length λ associated with the KT transition is also determined, and its temperature dependence is found to be different from the behavior of ξ, but in good agreement with Kosterlitz' result, Eq. (14).[23]

We finally turn to the behavior of ξ at $T<T_c$. At these temperatures we have no data with $\Upsilon\approx0$, (and if we had, there might also be a problem fulfilling $L\gg\xi$) and we therefore need some other methods to avoid the finite-size effects. The solution is to restrict the analysis to $T\lesssim T_{\mathrm{KT}}$, where the different boundary conditions of Sec. II F may be employed. However, the temperature dependence of ξ below T_c (and T_{KT}) does not seem to be useful for assessing the critical behavior, possibly an effect of the presence of the KT transition between the obtained data and T_c.

A. The correlation length in the 2D Ising model

The Hamiltonian of the Ising model is

$$H^I=-J\sum_{\langle ij\rangle}s_is_j,$$

where i and j numerate the lattice points, $s_i=\pm1$, and the summation is restricted to nearest neighbors. In two dimensions the correlation length exponent is $\nu=1$, and at a square lattice the critical temperature is known to be

$$T_c^I/J=\frac{2}{\ln(\sqrt{2}+1)}\approx2.269.$$

Since $\nu=1$, a plot of $1/\xi$ versus T is expected to yield a rectilinear behavior down to T_c^I. However, the verification of this turns out to require data fairly close to T_c^I, large correlation lengths, and therefore rather big lattices. For most pur-

poses this exercise is pointless, since—beside being obtained from the exact solution—the value $\nu=1$ may be verified from MC simulations by means of finite-size scaling at T_c^I. But since this kind of finite-size scaling does not seem to work in the FFXY models for the accessible lattice sizes, we have to resort to analyses of the correlation functions. With that background, analyses of the correlation function for the 2D Ising model serves as a help to develop techniques for similar analyses of the FFXY model. Beside the benefit of the exactly known critical behavior, the analysis of the Ising model is greatly simplified by means of the cluster algorithm[30] that is instrumental in obtaining MC data with small statistical errors.

1. Determination of the correlation length

At first sight the obvious way to determine the correlation length is to examine the exponential decrease of the correlation function $g(r)$ down to zero. This amounts to adjusting the parameters A and ξ to obtain the best possible fit to the expression,

$$g(r)=Ae^{-r/\xi}.$$

At temperatures closely above T_c, the above expression should be modified to take correlations across the whole system into account. This is customarily done by instead fitting to an expression with the periodicity of the system,

$$g(r)=A(e^{-r/\xi}+e^{-(L-r)/\xi}). \tag{19}$$

It is, however, difficult to obtain reliable values for the correlation length with this procedure. The main complication is that the optimum value of ξ does depend on the range in r employed for the fit. This is not too surprising, since the pure exponential decay only is expected for very small values of $g(r)$.

An alternative determination of ξ by means of $g(k)$, the Fourier components of the correlation function, has been suggested in Ref. 34,

$$\xi=\frac{L}{2\pi}\sqrt{\frac{g(0)}{g(2\pi/L)}-1}. \tag{20}$$

An advantage with this expression is that no fitting is needed, and that the arbitrariness involved in choosing the fitting interval is eliminated. This expression may be derived from

$$g(\mathbf{k})\propto\frac{1}{\mathbf{k}^2+\xi^{-2}}. \tag{21}$$

The relation to an exponential decay is obtained since the Fourier transform of this function is the Bessel-K_0 function,

$$g(r)\propto K_0(r/\xi),$$

with the limiting behavior $\sim e^{-r/\xi}$.

In order to check that the determinations of ξ from Eq. (20) really do probe the long-distance limit, we have fitted $g(r)$ for $r_{\min}<r<2r_{\min}$ to Eq. (19), and examined the dependence of $1/\xi$ on $r_{\min}$. It turns out that, plotted versus $1/r_{\min}$, these points fall on close to a straight line, which as $1/r_{\min}\to0$ approaches the value of $1/\xi$ obtained from Eq.

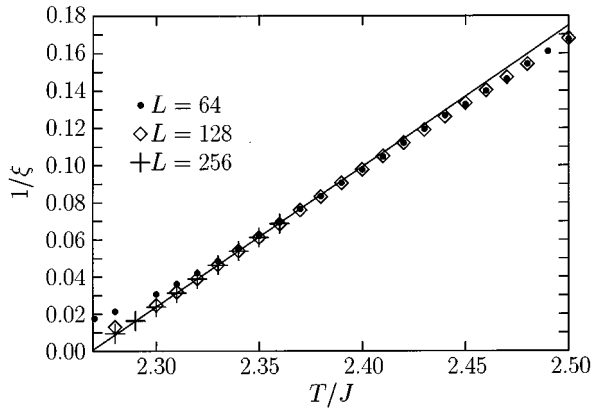FIG. 7. Correlation length in the 2D Ising model for $L = 64$, 128, and 256. The solid line is from fitting to Eq. (24) for $T/J \lesssim 2.33$ with data that fulfills $L/\xi > 5$.

(20). On the basis of this comparison we believe that Eq. (20) indeed does give a reliable way to determine the correlation length ξ.

A precise determination of ξ with Eq. (20) requires fairly long MC simulations. This is the case since $g(2\pi/L)$ and $g(0)$ measure the amplitude of the largest fluctuations in the system, with the correspondingly long decorrelation times. A way to reduce the effect of statistical errors is to include some more k vectors in the analysis. This is motivated by the difficulty to obtain good accuracy from Eq. (20) on data from the FFXY model at large lattices ($L = 128$, 256). However, using $g(k)$ in a too large interval will affect the correlation length ξ. Assuming that the exponential r dependence only holds for $r \gg \xi$, or, similarly, that the asymptotic k dependence only is valid for $k \ll 2\pi/\xi$, we restrict ourselves to making use of data from wave vectors $k < \pi/\xi$, only. For small values of ξ this is not very restrictive, and since we are interested in the small-k limit we impose the additional condition $k < \sqrt{0.1}$.

The procedure to determine ξ is then to first fit the data to

$$\frac{1}{g(\mathbf{k})} = g_0 + g_1 \widetilde{\mathbf{k}}^2 + g_2 (\widetilde{\mathbf{k}}^2)^2, \qquad (22)$$

(where we also include a second-order term in $\widetilde{\mathbf{k}}^2$ to take care of the curvature in the data) and then extract the correlation length through

$$\xi = \sqrt{g_1/g_0}. \qquad (23)$$

In the limiting case with only two wave vectors, this procedure is readily shown to be equivalent to Eq. (20).

2. Determination of the critical behavior

Figure 7 shows the temperature dependence of the correlation length in the 2D Ising model for three different system sizes, $L = 64$, 128, and 256. In the vicinity of T_c^I the data reveals some finite-size effects. The correlation length becomes smaller in a too small system. The present data seems to suggest that the determinations are reliable only if $L/\xi > 5$.

Also apparent in the figure is a slight curvature in the data. The expected linear behavior is found only right above
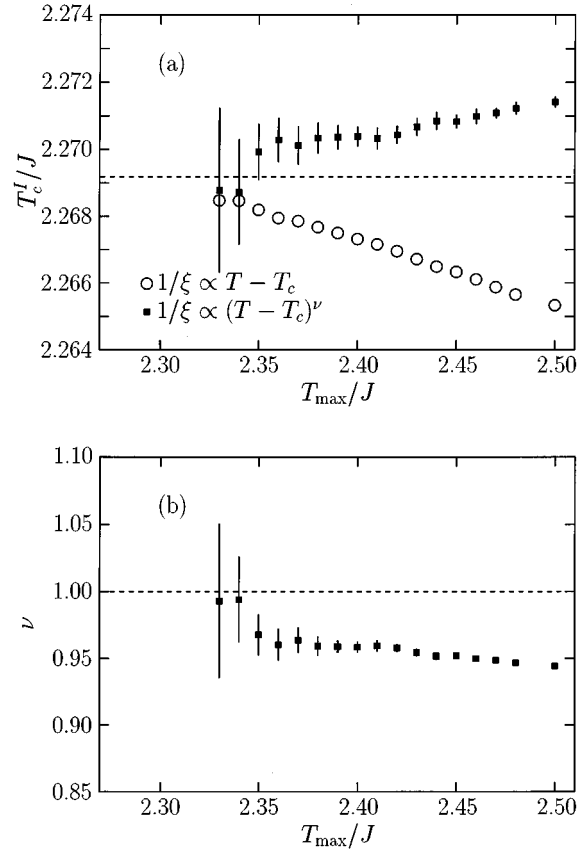

FIG. 8. Determinations of T_c and ν in the 2D Ising model from the correlation length data by fitting to Eqs. (24) and (25). The open circles are from fits with the exponent kept fixed, $\nu = 1$, whereas the solid squares are obtained with both T_c and ν as free parameters. The general trend is that both quantities approach the exact values, indicated by the dashed lines, as the temperature interval is decreased.

T_c^I. Estimates of T_c^I may be obtained by fitting

$$1/\xi = A(T - T_c), \qquad (24)$$

with A and T_c as free parameters. In these analyses we only make use of data for $L = 128$ and 256. Due to the curvature in the data, the critical temperature obtained in this way does depend on the temperature interval for the fit. For temperatures closely above T_c^I we only include data points with $L/\xi > 5$. This gives L-dependent lower limits for the temperature interval. The upper limit of the temperature interval is given by $T_{\max}$. The fit is then performed for several different values of $T_{\max}$. The dependence of T_c^I on $T_{\max}$ is shown by open circles in Fig. 8(a). The dashed line is the exact value of T_c^I. For large $T_{\max}$ (large temperature intervals) the analysis yields too low estimates of the critical temperature, but with decreasing $T_{\max}$ the estimated T_c^I increases towards the correct value.

This linear fit presumes a known value of the correlation length exponent ν. Since the value of ν in the FFXY model is highly disputed it is also of interest to perform the fit with ν as a free parameter. That is done by fitting
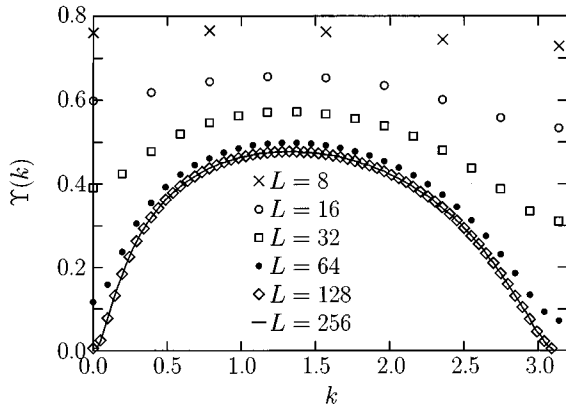
FIG. 9. Size dependence of $\Upsilon(\mathbf{k})$ at $T/J=0.840$ for $\mathbf{k}=(k_x,0)$. The message in this figure is that $\Upsilon(\mathbf{k})$ and thereby $g(\mathbf{k})$ is size dependent unless $\Upsilon(\mathbf{k}=0)=0$.

$$1/\xi = A(T-T_c)^\nu, \tag{25}$$

with ν, A, and T_c, as free parameters. Again we repeat the analysis for several different $T_{\max}$. The values of T_c^I and ν as functions of $T_{\max}$ are shown by solid squares in Figs. 8. We find that both quantities approach the expected values as the temperature interval is reduced. The erratic behavior at low values of $T_{\max}$ is due to statistical errors that become significant in such narrow temperature intervals.

B. Finite-size effects

In the previous section we found, much as expected, that it is necessary to perform the MC simulations of the 2D Ising model at systems that are considerably larger than the correlation length. The criterion was $L/\xi > 5$. When finite-size effects set in we get larger correlations and, thereby, a too small correlation length. In this section we demonstrate that in the analysis of the FFXY model, this condition has to be supplemented by a second one that is related to the additional XY degrees of freedom, and the corresponding screening length, λ. In terms of the helicity modulus this condition may be written $\Upsilon \approx 0$, which is equivalent to $L \gg \lambda$.

It turns out that $g(q)$ (and thereby also ξ) suffers from finite-size effects unless the system is large enough that $\Upsilon \approx 0$. This may be understood by examining the wave-vector-dependent helicity modulus $\Upsilon(k)$ for different system sizes. This is done in Fig. 9 and shows $\Upsilon(k)$ at $T/J=0.84$, well above both T_{KT} and T_c. Implicit in this discussion is the close relation between $g(\mathbf{k})$ and $\Upsilon(\mathbf{k})$ in Eqs. (5) and (6).

At each temperature above T_{KT} the helicity modulus $\Upsilon \equiv \Upsilon(k=0)$ vanishes for sufficiently large L. A finite value of Υ may therefore be considered a finite-size effect. The message of Fig. 9 is that if Υ suffers from finite-size effects, then the same is true for all the other components $\Upsilon(k)$, as well. The converse also appears to be true. For system sizes with $\Upsilon \approx 0$, $\Upsilon(k)$ is independent of L. This is illustrated by the two largest systems $L=128$ (diamonds) and 256 (solid line), with data just on top of each other.

From the relations between $\Upsilon(\mathbf{k})$ and $g(\mathbf{k})$ the above result is of relevance for $g(\mathbf{k})$. We therefore conclude that our results for the correlation function are without significant finite-size effects only if $\Upsilon \approx 0$, which means that precisely
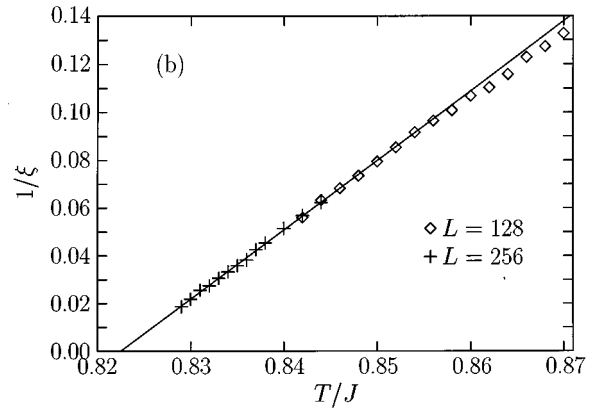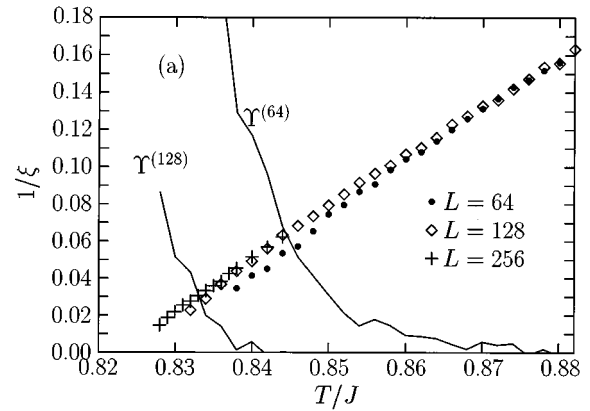

FIG. 10. Correlation length ξ in the FFXY model. (a) Examination of the finite-size effects. The data corroborates the conclusion that the determinations of ξ suffer from finite-size effects if $\Upsilon \neq 0$. (b) The correlation length data to be used in the determinations of T_c and ν. The solid line is obtained by fitting to Eq. (24) for $T \leq 0.842J$. Estimates of the statistical uncertainties in ξ are found in Table II.

this condition has to be fulfilled to facilitate reliable determinations of the correlation length ξ.

In the following determination of T_c and ν we only make use of the data for the larger lattices, $L=128$ and 256. For $L=128$ the criterion $\Upsilon \approx 0$ suggests making use of data for $T/J > 0.84$, only. The corresponding temperature limit for $L=256$ is more difficult to obtain since $\Upsilon^{(256)}$ suffers from large statistical errors. The temperature limit we have used, $T>0.828J$, is obtained by considering the fraction L/λ. The temperature limit for $L=128$ gives $(L/\lambda)_{\min} > 27$, which for $L=256$ is fulfilled only for $T/J > 0.828$. The determination of λ is discussed in Sec. IV D.

One should, of course, keep in mind that the usual finite-size effect, related to the fraction L/ξ, also may be relevant in these systems. It does, however, seem that this condition is the more restrictive one only for sizes $L>256$.

C. The correlation length in the FFXY model

We now apply the methods and results from the previous sections to our MC data for the FFXY model. Figure 10(a) shows our values for ξ obtained by self-consistently fitting $g(\mathbf{q})$ with $q < \pi/\xi$ and $q < \sqrt{0.1}$ to Eq. (22) for systems of size $L=64$, 128, and 256. The data for the larger sizes are

TABLE II. Correlation length versus temperature for system sizes $L=128$ and 256, together with rough estimates of the associated statistical errors. NMCS is the number of Monte Carlo sweeps through the system for the respective sizes. The data above the horizontal lines suffer from finite-size effects and are therefore not used in the determinations of T_c and ν in Sec. IV C.

T/J	$\xi^{(128)}$	NMCS/10^6	$\xi^{(256)}$	NMCS/10^6
0.828			68.2(2.4)	23
0.829			53.6(1.5)	23
0.830			45.8(1.5)	22
0.831			39.1(1.0)	18
0.832	43.9(1.9)	12	36.3(9)	18
0.833			32.6(8)	18
0.834	34.6(1.3)	8	30.0(6)	18
0.835			27.9(5)	18
0.836	27.1(5)	40	26.1(4)	18
0.837			23.5(3)	18
0.838	22.8(3)	58	22.0(3)	17
0.840	20.3(3)	56	19.4(2)	18
0.842	17.8(2)	56	17.6(2)	19
0.844	15.78(11)	92	16.0(2)	19
0.846	14.64(12)	64		
0.848	13.60(9)	64		
0.850	12.59(8)	64		
0.852	11.71(9)	32		
0.854	10.91(7)	40		
0.856	10.36(6)	40		
0.858	9.91(6)	40		
0.860	9.36(9)	16		
0.862	9.06(8)	16		
0.864	8.63(8)	16		
0.866	8.14(10)	9		
0.868	7.85(7)	16		
0.870	7.53(8)	10		

FIG. 11. Determinations of T_c and ν from the temperature dependence of ξ. This is a careful analysis of the data shown in Fig. 10(b) and listed in Table II. The fits are performed with several different temperature intervals, including data up to T_{max}. The open circles are obtained by fitting to Eq. (24), i.e., assuming that $\nu=1$. The solid squares are obtained with ν as a free parameter by fitting to Eq. (25). Panel (a) shows the obtained critical temperatures whereas panel (b) show the corresponding values of ν. This is very similar to the behavior in the 2D Ising model, shown in Fig. 8.

also given in Table II. Also shown is the helicity modulus for the two smaller sizes. We note that ξ for $L=64$ (solid dots) start to deviate from the results for the larger lattice ($L=128$, open squares) at the temperature where $\Upsilon^{(64)}$ becomes appreciably different from zero. The corresponding situation holds for ξ obtained with $L=128$ and 256. Note also that this finite-size effect is somewhat peculiar since analysis of data from a smaller lattice yields a *too large* value of the correlation length. This is opposite to the usual case, cf. Fig. 7.

After skipping the data affected by finite-size effects, the analysis of the correlation function in the FFXY model, becomes very similar to the corresponding analysis of the 2D Ising model in Sec. IV A. The data to be used is shown in Fig. 10(b).

For determinations of T_c we first assume $\nu=1$ and fit our data to Eq. (24) for temperatures $T \lesssim T_{max}$. Our results for the critical temperature vs T_{max}, are shown as open circles in Fig. 11(a). The figure shows a slowly increasing trend in T_c for decreasing T_{max}, similar to the results for the Ising model, Fig. 8(a). From this we get our best value of the Z_2 temperature, $T_c/J \approx 0.8225(5)$. The line in Fig. 10(b) is from the fit with $T_{max}/J = 0.842$.
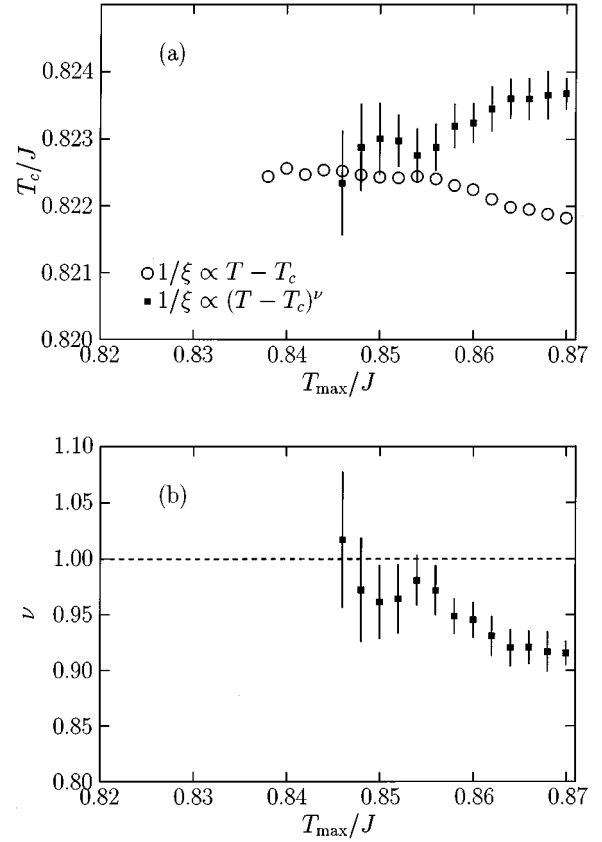
The next step is to do a similar fit with ν as a free parameter, by fitting to Eq. (25). Our values of T_c and ν are shown by solid squares as functions of T_{max} in Fig. 11. For large T_{max} the analysis gives non-Ising exponents, $\nu \approx 0.9$, but as T_{max} decreases (the temperature interval shrinks) the data suggest an increasing trend in ν towards 1.0. From this analysis of the temperature dependence of ξ we therefore conclude that the data, indeed, is consistent with $\nu=1$.

We also note that this dependence of ν on T_{max} is very similar to the corresponding analysis in the 2D Ising case, Fig. 8(b). Analyses based on data from a somewhat too large temperature interval suggested $\nu<1.0$, but with decreasing temperature interval the correct value of the exponent was obtained. This comparison serves to strengthen our conclusion of the ordinary 2D Ising value for the correlation length exponent in the FFXY model.

D. Screening length λ

It is also of great interest to determine the screening length λ, associated with the free vortices in the system. This turns out to, in some respects, be similar to the above deter-
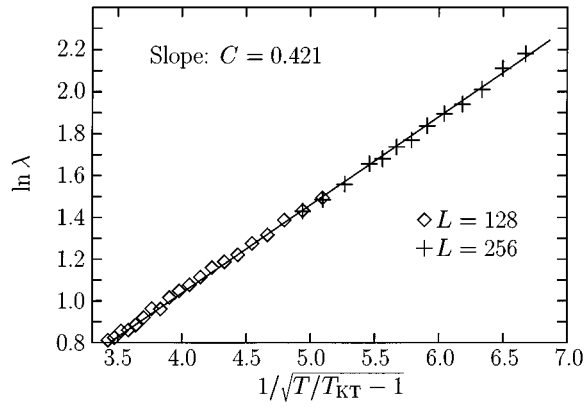
FIG. 12. Verification of the Kosterlitz temperature dependence for λ. Here $T_{KT}/J = 0.8108$ from Sec. III D and the data affected by finite-size effects is removed. The slope from this figure is, however, not in accordance with $C = 0.54 \pm 0.02$ from the finite-size scaling analysis in Sec. III D.

mination of ξ. The starting point is the expected behavior for the wave-vector-dependent helicity modulus,[22]

$$\Upsilon(\mathbf{k}) \equiv \frac{J}{\epsilon(\mathbf{k})} = \frac{J}{\widetilde{\epsilon}} \frac{\widetilde{\mathbf{k}}^2}{\widetilde{\mathbf{k}}^2 + \lambda^{-2}},$$

where λ is the screening length associated with free vortices and $\widetilde{\epsilon}$ is due to the polarization of bound pairs.[22] Neglecting the k dependence in $\widetilde{\epsilon}$ one expects $\widetilde{\mathbf{k}}^2/\Upsilon(k)$ to be linear in $\widetilde{\mathbf{k}}^2$. This is, however, not quite the case. The data shows a negative curvature and we therefore perform a fit to the second-order polynomial

$$\frac{\widetilde{\mathbf{k}}^2}{\Upsilon(k)} = a_0 + a_1 \widetilde{\mathbf{k}}^2 + a_2 (\widetilde{\mathbf{k}}^2)^2.$$

Assuming that the above equation holds for wavelengths larger than λ we, self-consistently, make use of data for $k < \pi/\lambda$, only. The screening length is then obtained from $\lambda = \sqrt{a_1/a_0}$.

The screening length obtained in this way does indeed fit well to the well-known Kosterlitz expression for the characteristic length.[23] This is shown in Fig. 12 where we plot $\ln\lambda$ vs $1/\sqrt{T/T_{KT} - 1}$. From this linear curve it is possible to get an approximate value for the screening length at T_c. An extrapolation to $T_c/J = 0.8225$ gives $\lambda(T_c) \approx 17.7$. From our rough criterion for negligible finite-size effects in Sec. IV C, $L/\lambda > 27$, we may then estimate that the finite-size effects at T_c associated with the nearby KT transition would be negligible for systems with $L > 480$.

The slope $C \approx 0.42$ is not quite in accordance with $C \approx 0.54$ obtained from the finite-size analysis of Υ_L in Sec. III D. This kind of difference was also found in the ordinary XY model with no frustration.[27] However, it is only the analysis in Sec. III D that probes the region immediately around T_{KT}, and this appears therefore to be the more reliable one when it comes to determining the asymptotic behavior.
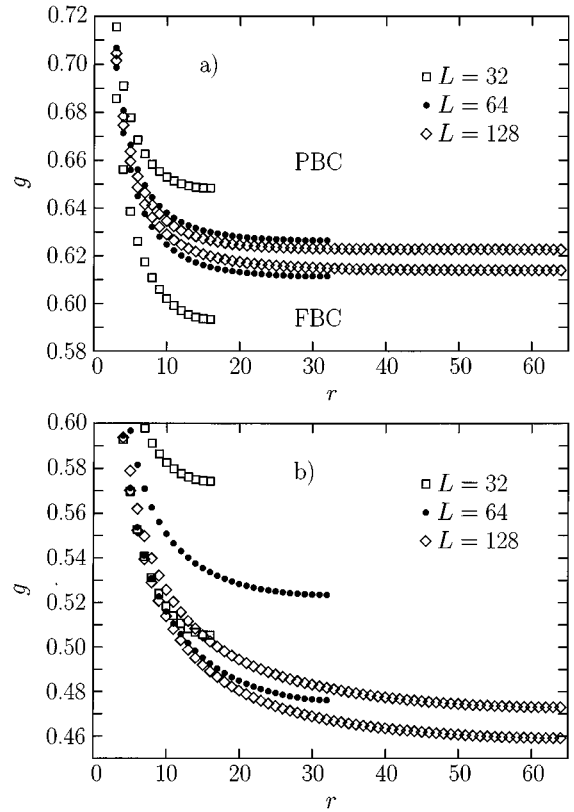

FIG. 13. The correlation function $g(r)$ with different boundary conditions. Panel (a) is for $T = 0.81J \approx T_{KT}$, whereas panel (b) is for $T_{KT} < T = 0.82J < T_c$. At the lower temperature the correlation functions obtained with the two different boundary conditions scale with the system size in opposite ways, which facilitates a determination of the behavior in the thermodynamic limit. At the higher temperature this is no longer true and there is no easy way to extrapolate to the behavior in the thermodynamic limit.

E. Different boundary conditions

Figures 13 show $g(r)$ versus r at $T/J = 0.81$, and 0.82, respectively, obtained with both PBC's and FBC's for lattice sizes $L = 32$, 64, and 128. At the lower temperature the results from larger lattices are squeezed in between the PBC and FBC results for a smaller system. When this behavior is valid, it seems safe to conclude that the behavior of an infinite system is somewhere between these two limits, and, to an excellent approximation, may be obtained as the average of these two curves.

The behavior is dramatically different at the higher temperature. This is the case even though this temperature is well below T_c. (We expect this different behavior to set in for $T > T_{KT}$.) At this higher temperature, $g(r)$ for both PBC's and FBC's decrease with increasing lattice size, and it is therefore not possible to obtain any safe estimate for the behavior in the thermodynamic limit.

We are now in the position to determine $M_\infty(T_{KT})$. This is of great interest since our argument for two distinct transitions in Sec. III C 2 was based on a simple way to estimate this quantity. Our values for $M_\infty(T)$ are obtained by taking the average between data from PBC's and FBC's. M_∞ obtained in this way is shown in Fig. 14. With $T_{KT}/J = 0.8108$ we find $M_\infty(T_{KT}) \approx 0.783(2)$, which, indeed,
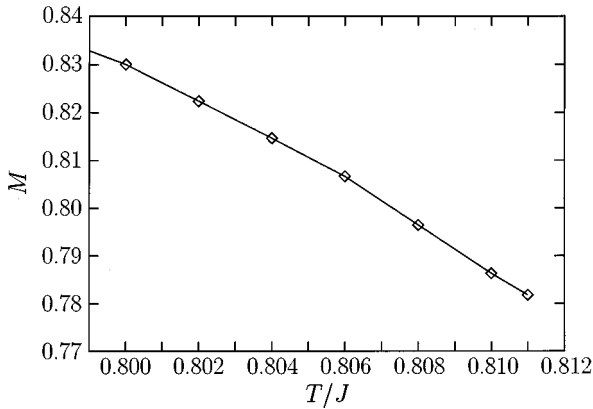
FIG. 14. The staggered magnetization. The figure shows the average of values obtained with PBC's and FBC's for $L=128$. Since these sets of values are very close (difference <0.01) we expect this average to be an excellent approximation of the behavior in the thermodynamic limit.

FIG. 15. The Z_2 correlation length ξ in the temperature region below T_c (and T_{KT}). Because of the dramatic change in the system at the KT transition, the critical temperature may not be determined from this kind of data.

is a good candidate to the $L \rightarrow \infty$ limit in Fig. 2. The results from our more elaborate analyses are thus in very good agreement with the simple approach of Sec. III C 2.

F. The correlation length ξ for $T < T_c$

In this section we focus on the Z_2 correlation length in the low-temperature region, $T < T_c$. As discussed above we actually need $g(q)$ for an infinite system for a reliable determination of ξ. As shown in Fig. 13(a) the finite-size effects may be virtually eliminated by taking the average of $g(r)$ for PBC's and FBC's. The same turns out to be true for the Fourier components $g(q)$. However, as discussed above this only works at $T < T_{KT}$, which means that it does not seem possible to get any values for ξ right below T_c.

The starting point for the present analysis is MC data obtained with both PBC's and FBC's for a lattice of size $L=128$, in a temperature interval $0.770 \le T/J \le 0.811$. Much as in Sec. IV C we fit $1/g(q)$ to an expansion in $\widetilde{\mathbf{q}}^2$, cf. Eq. (22). The data should be taken at small q; we restrict the analysis to $q < \sqrt{0.1}$. The main difference compared to the high-temperature case, is that the data for $q=0$ has to be excluded at low temperatures. This is so since $g(q=0)$ is directly related to the staggered magnetization squared and $g(q)$ therefore is not a smooth function at $q=0$, in the low-temperature phase.

Figure 15 shows the obtained values of ξ. There are two things to note. First, the data fall to a good approximation on a straight line, $1/\xi \propto (T-T^*)$, but with the temperature T^* significantly different from $T_c \approx 0.8225J$. The reason for this is possibly that T_{KT} lies between this data and T_c, and the system undergoes a dramatic change at the KT transition.

The second point of interest is the value of the correlation length at T_{KT}. The finite-size scaling analysis of Υ in Sec. III D would not be reliable if there were significant finite-size effects associated with the Z_2 degrees of freedom. We therefore need data with $L \gg \xi$. From Fig. 15 we find $\xi(T_{KT}) \approx 7.2$ which means that the systems used in the finite-size scaling analysis, indeed, are considerably larger than the correlation length; $L/\xi \gtrsim 4.4$ for the smallest system, $L=32$.
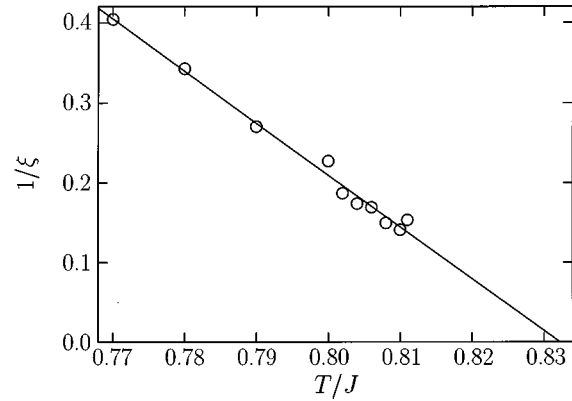
V. DISCUSSION

Our conclusion for the FFXY models with Villain or cosines[17] interaction is thus that there are two distinct transitions, with $T_{KT} < T_c$. This is in contrast to the conclusions from a study of frustrated systems with a variable bond strength $-\eta J$ at one bond per plaquette.[18] Here $\eta=1$ corresponds to the fully frustrated case, and both smaller and larger values of η were used in order to separate the transitions, with the hope that this information would shed light on the behavior of the FFXY model, $\eta=1$. The conclusions—Fig. 7 in Ref. 18—were that as η increases above $\eta_c=1/3$ there are two distinct transitions—with $T_c < T_{KT}$—which merge (or nearly so) at $\eta=1$. As η is increased further the transitions separate again, still with the Ising-like transition at the lower temperature.

Since the result at $\eta=1$ were not precise enough to exclude two distinct transitions, it is perfectly possible to harmonize these results with our present finding ($T_{KT} < T_c$ for $\eta=1$). The resulting picture is then the following. As a function of η the temperatures T_{KT} and T_c approach each other, cross at η below but close to 1, cross again above but close to $\eta=1$ and then separate as η increases. While this might be an unexpected scenario, it seems to be consistent with the conclusions based on the XY Ising model in Ref. 35.

To summarize the findings of the present paper, we have found ample evidence for two distinct transitions with $T_{KT} < T_c$ in the Villain version of the FFXY model. Our results corroborate the conclusions presented in Ref. 17. We have given a strong argument for two distinct transitions based on the universal jump condition alone, which amounts to demonstrating that the staggered magnetization is finite, and actually quite large, at the KT transition. Since this result is obtained with no complicated analysis or detailed fitting whatsoever, we consider this to be a very robust argument for the existence of two transitions in the FFXY model.

A detailed finite-size scaling analysis of the helicity modulus gives at hand that the model undergoes an ordinary KT transition at $T_{KT}/J=0.8108(1)$, and also that the size dependence of this quantity in narrow regions both below and above T_{KT} is just as expected for a KT transition. Furthermore, with this value for T_{KT} it is found that the tem-

perature dependence of the screening length is in accordance with the well-known Kosterlitz' expression.

From thorough studies of the correlation functions in both the FFXY model and the 2D Ising model, we have determined ξ and the correlation length exponent ν. Our studies show that the obtained values of ν depend on the size of the temperature intervals from which ξ are taken, and that ν approaches 1.0 as the size of the temperature interval is decreased. The result is therefore clearly in favor of ordinary Ising exponents in the FFXY model. Using $\nu=1$ the Z_2 critical temperature was determined to $T_c/J=0.8225(5)$.

ACKNOWLEDGMENTS

APPENDIX: DUALITY TRANSFORMATION FOR A FRUSTRATED MODEL

The exact duality transformation[20] of the XY model with Villain interaction is between the XY model with PBC's and the Coulomb gas with a term proportional to the polarization squared.[21,11] The derivation and notations below closely follows Ref. 11. For an arbitrary set $\{A_{ij}\}$ the partition function is

$$Z=\int_{-\pi}^{\pi} \prod_l \frac{d\theta_l}{2\pi}\exp\left(-\beta\sum_{\langle ij\rangle} U(\theta_i-\theta_j-A_{ij})\right). \quad (A1)$$

With the Fourier expansion of the Boltzmann factor

$$e^{-\beta U(\phi)}=\sum_{h=-\infty}^{\infty}\frac{e^{-h^2/2\beta J}}{\sqrt{2\pi\beta J}}e^{ih\phi},$$

the partition function becomes

$$Z=\sum_{\{h_{ij}\}=-\infty}^{\infty}\exp\left(i\sum_{\langle ij\rangle}h_{ij}A_{ij}\right)\int\prod_l\frac{d\theta_l}{2\pi}$$

$$\times\exp\left(i\theta_l\sum_{j\in\langle jl\rangle}h_{jl}\right)\prod_{\langle ij\rangle}\frac{e^{-h_{ij}^2/2\beta J}}{\sqrt{2\pi\beta J}}.$$

Integration over θ_l gives restrictions on the set $\{h_{ij}\}$, $\Sigma_j h_{jl}=0$ for each l. A new set of variables, defined at the centers of the plaquettes, take care of these restrictions:

$$h_\mathbf{r}^x=S_{\mathbf{r}+\hat{\mathbf{y}}/2}-S_{\mathbf{r}-\hat{\mathbf{y}}/2},$$

$$h_\mathbf{r}^y=S_{\mathbf{r}-\hat{\mathbf{x}}/2}-S_{\mathbf{r}+\hat{\mathbf{x}}/2}, \quad (A2)$$

together with $\mathbf{S}=(S_x,S_y)$ which are included to allow for $\Sigma_\mathbf{r}h_\mathbf{r}^\mu\neq 0$, $\mu=x,y$.[11] To take care of the frustration we make use of $\mathbf{D}\times\mathbf{A_r}=2\pi f_\mathbf{r}$:

$$\sum_\mathbf{r} h_\mathbf{r}^x A_\mathbf{r}^x+h_\mathbf{r}^y A_\mathbf{r}^y=\sum_\mathbf{r}(S_{\mathbf{r}+\hat{\mathbf{y}}/2}-S_{\mathbf{r}-\hat{\mathbf{y}}/2})A_\mathbf{r}^x$$

$$+(S_{\mathbf{r}-\hat{\mathbf{x}}/2}-S_{\mathbf{r}+\hat{\mathbf{x}}/2})A_\mathbf{r}^y$$

$$=\sum_\mathbf{r} S_\mathbf{r}(A_{\mathbf{r}-\hat{\mathbf{y}}/2}^x-A_{\mathbf{r}+\hat{\mathbf{y}}/2}^x+A_{\mathbf{r}+\hat{\mathbf{x}}/2}^y-A_{\mathbf{r}-\hat{\mathbf{x}}/2}^y)$$

$$=\sum_\mathbf{r} S_\mathbf{r}(\mathbf{D}\times\mathbf{A_r})=2\pi\sum_\mathbf{r} S_\mathbf{r}f_\mathbf{r},$$

$$Z=\sum_{\{S_\mathbf{r}\},\mathbf{S}}\exp\left(i2\pi\sum_\mathbf{r} S_\mathbf{r}f_\mathbf{r}\right)\prod_{\langle\mathbf{r}\mathbf{r}'\rangle}\frac{e^{-[S_\mathbf{r}-S_{\mathbf{r}'}]^2/2\beta J}}{\sqrt{2\pi\beta J}},$$

using

$$\sum_S g(S)=\int d\sigma\sum_m e^{i2\pi m\sigma}g(\sigma),$$

this becomes

$$Z=\int\prod_\mathbf{r} d\sigma_\mathbf{r}d\boldsymbol\sigma\exp\left(-\sum_{\langle\mathbf{r},\mathbf{r}'\rangle}\frac{[\sigma_\mathbf{r}-\sigma_{\mathbf{r}'}]^2}{2\beta J}\right)$$

$$\times\sum_{\{m_\mathbf{r}\},\mathbf{m}}\exp\left[i2\pi\left(\mathbf{m}\cdot\boldsymbol\sigma+\sum_\mathbf{r}(f_\mathbf{r}+m_\mathbf{r})\sigma_\mathbf{r}\right)\right],$$

where $\mathbf{m}=(m_x,m_y)$. After a Fourier transform this may be written

$$Z=\int\prod_{\mathbf{k}>0}(d\,\mathrm{Re}\sigma_\mathbf{k})(d\,\mathrm{Im}\sigma_\mathbf{k})d\boldsymbol\sigma\exp\left(\frac{1}{2\beta JL^2}\sum_\mathbf{k}\frac{|\sigma_\mathbf{k}|^2}{G(\mathbf{k})}-\frac{1}{\beta J}\frac{\boldsymbol\sigma^2}{2}\right)\sum_{\{m_\mathbf{r}\},\mathbf{m}}\exp\left(\frac{2\pi^2\beta J}{L^2}\sum_\mathbf{k} G(\mathbf{k})|m_\mathbf{k}+f_\mathbf{k}|^2-2\pi^2\beta J\mathbf{M}^2\right),$$

$$(A3)$$

where $\mathbf{M}=\mathbf{m}+(1/L)\Sigma_\mathbf{r}m_\mathbf{r}\mathbf{r}$ is the polarization. After a transformation back to ordinary space, this gives

$$Z=Z_{\mathbf{sw}}\sum_{\{m_\mathbf{r}\},\mathbf{m}}\exp\left[-4\pi^2\beta J\left(-\frac{1}{2}\sum_{\mathbf{r},\mathbf{r}'}(m_\mathbf{r}+f_\mathbf{r})G(\mathbf{r}-\mathbf{r}')(m_{\mathbf{r}'}+f_{\mathbf{r}'})+\frac{\mathbf{M}^2}{2}\right)\right].$$

Dropping the spin-wave part Z_{sw}, specializing to the frustration $f_{\mathbf{r}}=1/2$, and substituting $m_{\mathbf{r}}+f_{\mathbf{r}}\to m_{\mathbf{r}}$, we may then write

$$Z=\sum_{\{m_{\mathbf{r}}=\pm 1/2\ldots\},\mathbf{m}}$$
$$\times\exp\left[-4\pi^2\beta J\left(-\frac{1}{2}\sum_{\mathbf{r},\mathbf{r}'}m_{\mathbf{r}}G(\mathbf{r}-\mathbf{r}')m_{\mathbf{r}'}+\frac{\mathbf{M}^2}{2}\right)\right],$$
(A4)

which is our final result for the partition function.

We then turn to demonstrating the equivalence of Eqs. (6) and (7). The wave-vector-dependent helicity modulus is defined through[36]

$$\Upsilon(\mathbf{k})=L^2\frac{\partial^2 F}{\partial A_{\mathbf{k}}^x\partial A_{-\mathbf{k}}^x},$$

where the derivative is with respect to an $A_{\mathbf{k}}$ that is transverse, i.e., $\widetilde{\mathbf{k}}\cdot\mathbf{A}_{\mathbf{k}}=0$. Since only the rotation of $\mathbf{A}$ contributes to the change in free energy, we make use of $2\pi f_{\mathbf{k}}=i\widetilde{\mathbf{k}}\times\mathbf{A}_{\mathbf{k}}$ to obtain[37]

$$\Upsilon(\mathbf{k})=\frac{\widetilde{\mathbf{k}}^2}{4\pi^2}L^2\frac{\partial^2 F}{\partial f_{\mathbf{k}}\partial f_{-\mathbf{k}}}.$$

From Eq. (A3) then follows

$$\frac{1}{Z}\frac{\partial^2 Z}{\partial f_{\mathbf{k}}\partial f_{-\mathbf{k}}}$$
$$=\left\langle\frac{4\pi^2 J}{TL^2}G(\mathbf{k})\right\rangle$$
$$+\left\langle\left(\frac{4\pi^2 J}{TL^2}\right)^2|m_{-\mathbf{k}}+f_{-\mathbf{k}}|G(\mathbf{k})|m_{\mathbf{k}}+f_{\mathbf{k}}|G(-\mathbf{k})\right\rangle,$$

which, with $F=-T\ln Z$, $\widetilde{\mathbf{k}}^2=-1/G(\mathbf{k})$, and $m_{\mathbf{k}}+f_{\mathbf{k}}\to m_{\mathbf{k}}$, reproduces Eq. (6).

By instead starting from Eq. (A1) we find

$$\frac{1}{Z}\frac{\partial^2 Z}{\partial f_{\mathbf{k}}\partial f_{-\mathbf{k}}}=\left\langle-\beta\sum_{\mathbf{r}}U''(\phi_{\mathbf{r}})\left|\frac{dA_{\mathbf{r}}}{df_{\mathbf{k}}}\right|^2\right\rangle$$
$$+\left\langle\beta^2\sum_{\mathbf{r}}U'(\phi_{\mathbf{r}})\frac{dA_{\mathbf{r}}}{df_{\mathbf{k}}}\sum_{\mathbf{r}'}U'(\phi_{\mathbf{r}'})\frac{dA_{\mathbf{r}'}}{df_{-\mathbf{k}}}\right\rangle.$$

To evaluate the derivatives we have to choose $\mathbf{A}_{\mathbf{r}}$ such that $\mathbf{D}\times\mathbf{A}_{\mathbf{r}}=2\pi f_{\mathbf{r}}$. One choice that fulfills this is

$$\mathbf{A}_{\mathbf{k}}=\frac{2\pi}{\widetilde{\mathbf{k}}^2}f_{\mathbf{k}}(i\widetilde{k}_y,-i\widetilde{k}_x),$$

that gives

$$\frac{d\mathbf{A}_{\mathbf{r}}}{df_{\mathbf{k}}}=\frac{2\pi}{\widetilde{\mathbf{k}}^2 L^2}(i\widetilde{k}_y,-i\widetilde{k}_x)e^{i\mathbf{k}\cdot\mathbf{r}}.$$

Putting all this together and introducing the current $\mathbf{j}_{\mathbf{r}}=[U'(\phi_{\mathbf{r}}^x),U'(\phi_{\mathbf{r}}^y)]$, the wave-vector-dependent helicity modulus becomes

$$\Upsilon(\mathbf{k})=L^2\frac{\widetilde{\mathbf{k}}^2}{4\pi^2}\frac{\partial^2 F}{\partial f_{\mathbf{k}}\partial f_{-\mathbf{k}}}=\langle U''(\phi_{\mathbf{r}})\rangle-\frac{\beta}{L^2}\langle\mathbf{j}_{\mathbf{k}}\cdot\mathbf{j}_{-\mathbf{k}}\rangle,$$

and with $2\pi J v_{\mathbf{r}}=\mathbf{D}\times\mathbf{j}_{\mathbf{r}}\Leftrightarrow 2\pi J v_{\mathbf{k}}=i\widetilde{\mathbf{k}}\times\mathbf{j}_{\mathbf{k}}$, we finally obtain Eq. (7).

---

*Electronic address: olsson@tp.umu.se

[1] J. Villain, J. Phys. C **10**, 1717 (1977).

[2] S. Miyashita and H. Shiba, J. Phys. Soc. Jpn. **53**, 1145 (1984).

[3] J. M. Thijssen and H. J. F. Knops, Phys. Rev. B **37**, 7738 (1988).

[4] Y. M. M. Knops, B. Nienhuis, H. J. F. Knops, and H. W. J. Blöte, Phys. Rev. B **50**, 1061 (1994).

[5] E. Granato, J. M. Kosterlitz, J. Lee, and M. P. Nightingale, Phys. Rev. Lett. **66**, 1090 (1991).

[6] S. Teitel and C. Jayaprakash, Phys. Rev. B **27**, 598 (1983).

[7] T. Garel and S. Doniach, J. Phys. C **13**, 887 (1980).

[8] D. H. Lee, J. D. Joannopoulos, J. W. Negele, and D. P. Landau, Phys. Rev. B **33**, 450 (1986).

[9] G. S. Grest, Phys. Rev. B **39**, 9267 (1989).

[10] J.-R. Lee, Phys. Rev. B **49**, 3317 (1994).

[11] P. Olsson, Phys. Rev. B **52**, 4511 (1995).

[12] J. Lee, J. M. Kosterlitz, and E. Granato, Phys. Rev. B **43**, 11 531 (1991).

[13] S. Lee and K.-C. Lee, Phys. Rev. B **49**, 15 184 (1994).

[14] G. Ramirez-Santiago and J. V. José, Phys. Rev. B **49**, 9567 (1994).

[15] E. Granato and M. P. Nightingale, Phys. Rev. B **48**, 7438 (1993).

[16] M. P. Nightingale, E. Granato, and J. M. Kosterlitz, Phys. Rev. B **52**, 7402 (1995).

[17] P. Olsson, Phys. Rev. Lett. **75**, 2758 (1995).

[18] B. Berge, H. T. Diep, A. Ghazali, and P. Lallemand, Phys. Rev. B **34**, 3177 (1986).

[19] T. Ohta and D. Jasnow, Phys. Rev. B **20**, 139 (1979).

[20] J. V. José, L. P. Kadanoff, S. Kirkpatrick, and D. R. Nelson, Phys. Rev. B **16**, 1217 (1977).

[21] A. Vallat and H. Beck, Phys. Rev. B **50**, 4015 (1994).

[22] P. Minnhagen, Rev. Mod. Phys. **59**, 1001 (1987).

[23] J. M. Kosterlitz, J. Phys. C **7**, 1046 (1974).

[24] D. R. Nelson and J. M. Kosterlitz, Phys. Rev. Lett. **39**, 1201 (1977).

[25] P. Minnhagen and G. G. Warren, Phys. Rev. B **24**, 2526 (1981).

[26] H. Weber and P. Minnhagen, Phys. Rev. B **37**, 5986 (1988).

[27] P. Olsson, Phys. Rev. B **52**, 4526 (1995).

[28] K. Binder, Phys. Rev. Lett. **47**, 693 (1981).

[29] P. Olsson, Phys. Rev. Lett. **73**, 3339 (1994).

[30] U. Wolff, Phys. Rev. Lett. **62**, 361 (1989).

[31] The author is grateful to Dr. Mats Wallin for this insight.

[32] P. Olsson, Phys. Rev. Lett. **77**, 4850 (1996).

[33] Some values for this constant may be found in Table IV in Ref. 27.

[34] F. Cooper, B. Freedman, and D. Preston, Nucl. Phys. B **210**, 210 (1982).

[35] J. Lee, E. Granato, and J. M. Kosterlitz, Phys. Rev. B **44**, 4819 (1991).

[36] Ciordas and Teitel (unpublished).

[37] A closely related expression is the first equality in Eq. (B1) in Ref. 11.